

**Supplemental material for “Sliding Mechanisms in Multilayered
Hexagonal Boron Nitride and Graphene:
The Effects of Directionality, Thickness, and Sliding Constraints”**

SUPPLEMENTAL RESULTS AND DATA

Table SI summarizes the binding energy and interlayer distance of multilayered h -BN and graphene. As the number of layers increases from two to five, multilayered h -BN structures consistently exhibit AA' stacking mode as the most stable one, while multilayered graphenes favor AB stacking modes except the trilayer graphene (ABC stacking). Correspondingly, both the adhesion energy and the interlayer distance asymptotically resemble the bulk results for multilayered h -BN and graphene.

TABLE SI. Interlayer distance d (Å) and binding energy E_b (meV/atom) of multilayered h -BN and graphene. The number of layers (l) is shown in the first column.

layers	h -BN			graphene		
	mode	d	PBE+MBD	mode	d	PBE+MBD
$2l$	AA'	3.37	24.7	AB	3.37	22.8
	AB_1	3.32	24.2	AA	3.50	18.9
$3l$	$AA'A$	3.36	34.4	ABA	3.36	31.4
	$AA'B_1$	3.33	34.0	ABC	3.36	31.6
$4l$	$AA'AA'$	3.33	39.5	$ABAB$	3.36	36.1
	$AA'AB_1$	3.33	39.2	$ABAC$	3.36	36.0
$5l$	AA'	3.33	42.6	ABA	3.35	38.7
	AB_1	3.34	41.6	ABC	3.35	38.1
bulk	AA'	3.33	52.4	AB	3.34	48.2

Figure S1 show how sliding constraints affect the contribution from PBE and MBD interactions to sliding energies. Clearly, the MBD interactions make a crucial contribution to the minimum energy pathways (S_X) of bilayer h -BN and graphene. In the S_{XY} and L_{XY} pathways of bilayer h -BN and graphene, the PBE contribution is found to be more important than in the S_X pathway. With the fully constrained top layer of bilayer h -BN (S_{XYZ} and L_{XYZ}), the PBE contribution, instead of MBD, dominates the sliding energy profile.

Table SII summarizes the thickness-dependent sliding barrier of multilayered h -BN and graphene. Overall, the interlayer sliding properties of multilayered h -BN are comparable

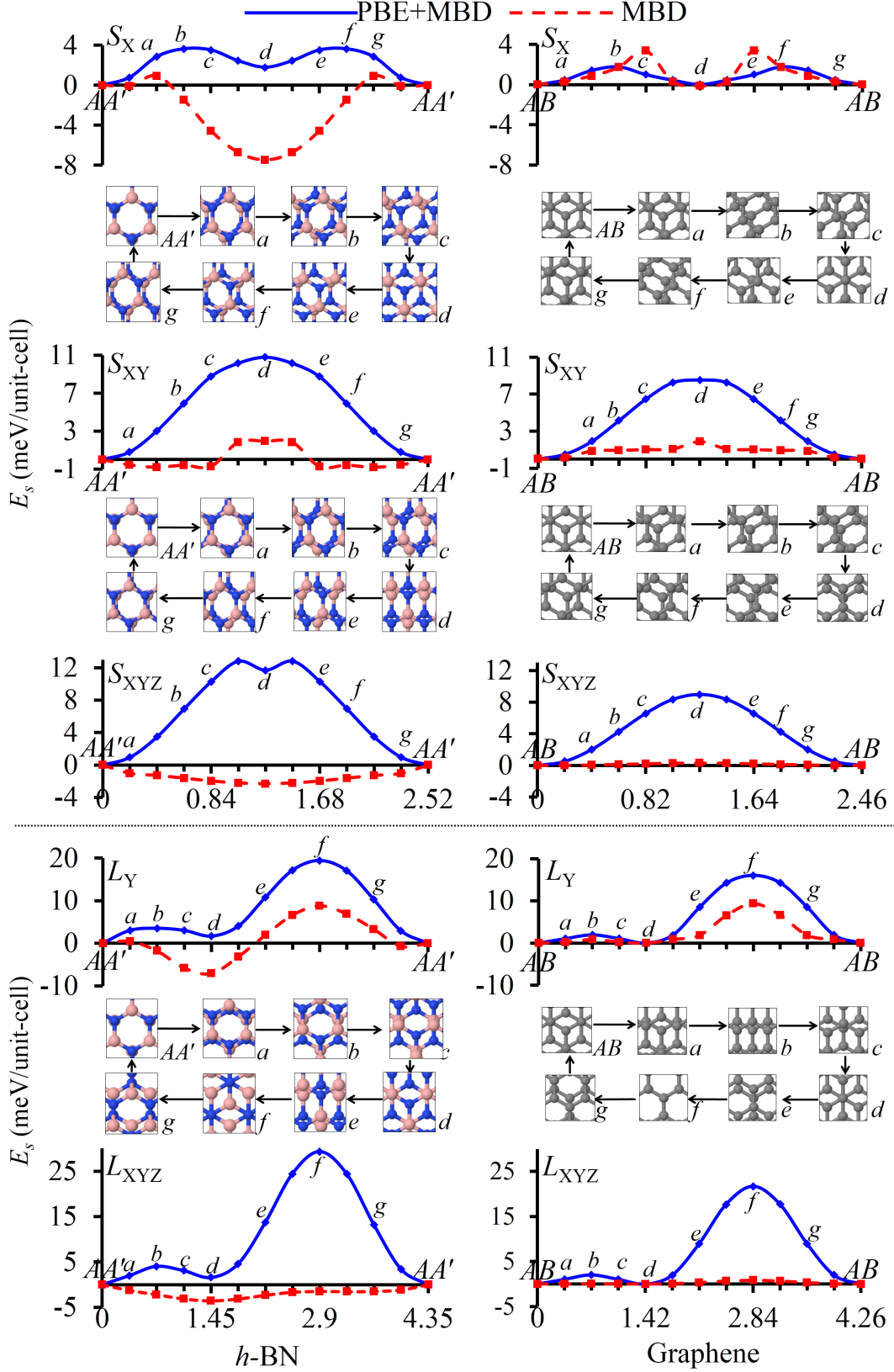


FIG. S1. Sliding energies E_s of the different S and L pathways for bilayer BN and graphene. The insert figures are the geometry of the selected configurations along the considered pathways for bilayer h -BN and graphene.

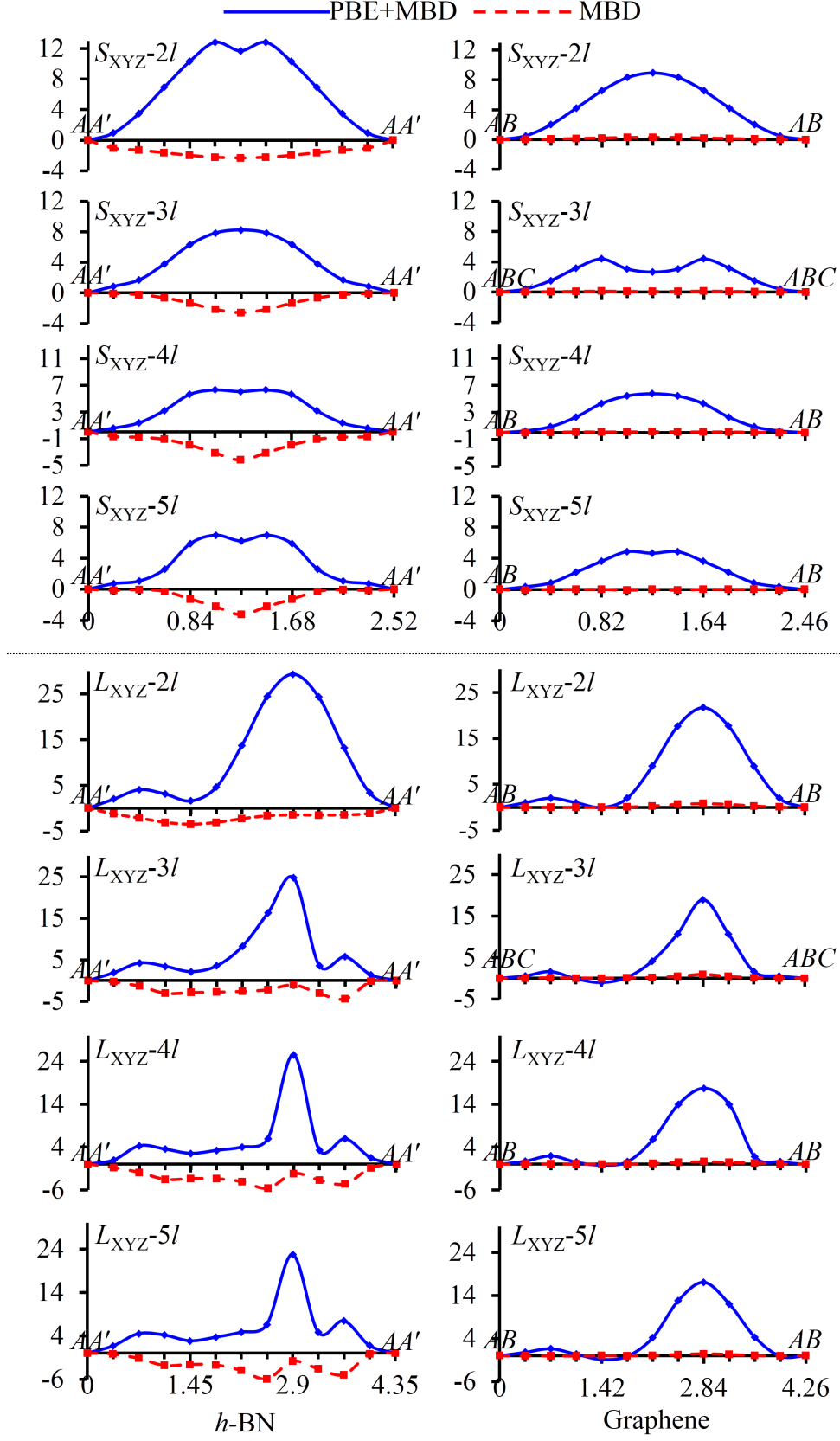


FIG. S2. Sliding energy profiles of the S_{XYZ} and L_{XYZ} pathways for multilayered h -BN and graphene in terms of the number of layers.

TABLE SII. Sliding barrier E_a of layered h -BN and graphene in different pathways (meV/unit-cell). a and b indicate the $E_{a,\text{tot}}$ (tot=PBE+MBD) and $E_{a,\text{MBD}}$ contribution, respectively.

layers	L_Y		L_{XYZ}		S_X		S_{XY}		S_{XYZ}	
h -BN	a	b	a	b	a	b	a	b	a	b
2l	19.4	9.5	29.3	3.5	3.6	8.4	10.8	2.7	13.8	2.3
3l	19.3	17.6	22.6	4.4	5.3	7.8	12.0	2.1	8.2	2.6
4l	19.0	14.1	21.0	4.6	5.0	8.3	11.9	2.0	6.3	4.2
5l	18.8	13.8	19.8	5.0	5.3	9.5	12.1	2.4	6.8	3.2
graphene	a	b	a	b	a	b	a	b	a	b
2l	16.0	9.4	21.7	0.8	1.8	3.5	8.5	1.9	9.0	0.3
3l	16.9	16.2	19.0	0.9	3.7	3.0	9.1	3.7	4.4	0.1
4l	15.9	19.0	17.9	0.6	3.8	2.8	8.7	2.9	5.5	0.1
5l	15.9	26.9	17.9	0.4	1.8	4.5	7.0	3.6	4.9	0.1

to those of multilayered graphene. In the S_X pathway of multilayered h -BN, the sliding barrier is first increased from 3.6 to 5.3 meV/unit-cell and then remains almost unchanged when increasing the number of layers. Importantly, the MBD interactions are competing with PBE in determining the sliding barrier. In the S_{XY} pathway of multilayered h -BN, the sliding barrier behaves in a similar way to that of the S_X pathway as the number of layers increases, while PBE energy dominates the sliding barrier (Table SII). Interestingly, the sliding barrier of the S_{XYZ} pathway basically decreases when increasing the number of h -BN layers (Figure S2). Without intermediate layers, the top layer of bilayer h -BN slides along the S_{XYZ} pathway with $E_{a,\text{tot}} = 13.8$ meV/unit-cell. With intermediate layers acting as a lubricant, the sliding barrier of the S_3 pathway becomes smaller. For thicker structures, more degrees of freedom are involved in the sliding process, leading to smaller overall sliding barriers. These conclusions are found to also hold for the L -associated pathways of layered h -BN (Table SII).

Table SIII summarizes the sliding distance that corresponds to sliding barrier for multilayered h -BN and graphene in S_{XYZ} and L_{XYZ} pathways. Clearly, the sliding distance depends on the number of layers, which can be seen from the sliding potential of S_{XYZ} and

L_{XYZ} pathways in Figure S2.

TABLE SIII. Sliding distance associated with sliding barrier for multilayered h -BN and graphene in S_{XYZ}/L_{XYZ} pathways (\AA).

	path	$2l$	$3l$	$4l$	$5l$
h -BN	S_{XYZ}	1.05	1.26	1.05	1.05
	L_{XYZ}	1.45	1.45	1.45	1.45
graphene	S_{XYZ}	1.23	0.82	1.23	1.03
	L_{XYZ}	1.42	1.42	1.42	1.42